Master's Thesis

Decoding Motor Commands in Cortico-Basal Ganglia Circuits for the Purpose of Controlling a Neuroprosthetic Device

Moa Svensson
Joel Sjöbom

Department of Electrical and Information Technology,
Faculty of Engineering, LTH, Lund University, January 2014.

Master Thesis

Decoding Motor Commands in Cortico-Basal Ganglia Circuits for the Purpose of Controlling a Neuroprosthetic Device

Moa Svensson and Joel Sjöbom

Neuronano Research Center

Advisors: Per Petersson and Ulrike Richter

February 19, 2014

Printed in Sweden
E-huset, Lund, 2014

Chapter 1

Abstract

Movement in vertebrates depends on neural activity in the motor regions of the brain such as the motor cortex and basal ganglia. This master thesis demonstrates the possibility to predict movement through computer learning. Different information is processed in different type of neurons, of which the neuron types medium spiny neurons (MSN) and fast spiking interneurons (FSI) from the striatum (an input structure of the basal ganglia), and pyramidal neurons (PN) and interneurons (IN) from the motor cortex have been analysed. The neural data was sorted with the software Offline sorter. 27 MSN's, 11 FSI's, 50 PN's and 7 IN's was classified depending on the characteristic features of the waveforms. 10 neurons remained unidentified. Refinements of video recordings were done in MATLAB toolbox BehaviourGUI developed by Neuronano Research Center (NRC). A total of 549 movement bouts was tracked across the video recordings.

A visual inspection of the neurons' perievent time histograms show that 12 out of 33 identified neurons in the striatum are clearly correlated to movement while only 8 out of 63 were clearly correlated in the motor cortex.

The motor commands were predicted by a computer learning program which utilises a linear model. The model has inputs of neuronal firing rates at a given time and time lag with weighted parameters depending on how important the neuron's firing rate is at each lag. The neurons' firing rate can be used to predict when the rat moves with relatively good precision.

Significant improvements might be done by making a more advanced prediction algorithm. Furthermore, better electrodes need to be used to record more accurate neural signals, and more neural data connected with movements need to be collected from the same vertebrate. What would also be of interest are recordings from other areas in the basal ganglia.

Table of Contents

List of Figures

List of Tables

Chapter 2
Prologue

Working with this project has been an exciting journey. Exciting because there is so much that remains unknown about the brain, so much knowledge waiting to be explored. Both of us were interested in getting a deeper knowledge of neuroscience and how the brain works. To get to examine it from an engineering perspective was of particular interest.

In this study we have focused on getting knowledge about the regions of the brain that control voluntary movement. New studies have been of great importance in getting a better insight within neuroscience. Therefore, we have tried to use the latest research, even though what is thought to be known changes quickly and might be outdated within a few years. Apart from how the motoric region of the brain works we have got a deeper knowledge of the techniques used to record and process the brain's signals.

Joel Sjöbom
Moa Svensson

Chapter 3
Introduction

The brain is a fascinating organ and yet little is known about how it works. This structure of one and a half kilogram allows us to think, be inspired, feel happiness and dream. It also controls our senses such as vision, hearing and movements.

Different parts of the brain specialise in different tasks. Each part can be seen as an island connected to other parts of the brain using bridges. Some bridges have two-way traffic while others are solely one-way. The traffic is electro-chemical signals, and decoding these signals are of especially great interest. Gaining access and understanding of these signals would be a momentous achievement for a multitude of medical research. A person with no legs, for example, could get a bionic pair of legs, controlled by the person's own thoughts, thereby restoring full freedom of movement. Such devices controlled directly by the brain are called neuroprosthetics. Finding the signals that could control locomotion (i.e. walking) via such a device is the ultimate goal of this project.

In the following chapter there will be a short review of how the neural system works with focus on the regions controlling locomotion; what the challenges are involving the creation of a communication pathway between brain and device; and the ethics when animals are involved in experiments.

3.1 Neurons and Neural Signals

In order to interpret a neural signal, it is of great importance to know more about: the anatomical structure of neurons; how a nerve impulse is produced and what the impulse signal looks like.

The primary components of the neural system in the brain are two cell types: neurons and glial cells. Neurons form and transmit signals, while glial cells protect, stabilize, and support the neuron [Purves et al.].

A neuron consists of three important parts: axons, dendrites and soma (Figure 3.1). The axon connects to muscles or to dendrites of other neurons via synapses; a special structure which makes it possible to electrochemically transmit signals from a so-called presynaptic neuron to another postsynaptic neuron. Some axons are covered with a shealth of myelin that improves the signal speed. The dendrites receive the signals from other neurons and lead them to the soma; the neuron's nucleus. If the combined input signals to the soma overcome a specific threshold

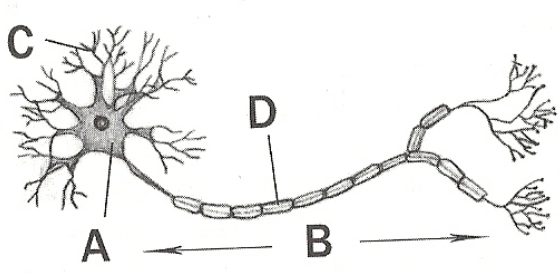

Figure 3.1: *Overview of the neuron's structure. A: Soma, B: Axon, C: Dendrites and its branchlets D: Myelin [Al-Chalabi et al.].*

the neuron sends a signal called an action potential. The action potential travels along the axon, and onto further neurons [Purves et al.].

In the absence of signalling, the potential difference between the inner and outer membrane of a neuron is about 70 mV, known as the neuron's resting potential. When a signal is received from another neuron, the cell membrane changes its potential to a lower or higher value, depending on whether the synapse is so-called inhibitory or excitatory [Purves et al.]. In Figure 3.2 the effect of inhibitory and exitatory input on the neuron's membrane potential can be seen. If the threshold for firing an action potential is exceeded and the membrane potential sharply rises to +20 mV. After an action potential is initiated, there is not a high probability that a second action potential is initiated during a certain refractory period [Purves et al.].

In more detail, inhibitory post-synaptic potentials (IPSP's), lower or hyperpolarize the membrane potential, which leads to a bigger gap between the current membrane potential and the threshold for eliciting an action potential. Excitatory post-synaptic potentials (EPSP's) increase or depolarize the membrane potential towards the threshold so an action potential is easier to achieve. Figure 3.2 shows on the left a sketch when an electrode records the post-synaptic potential in the soma of a neuron with two excitatory synapses (ES1 and ES2) and one inhibitory

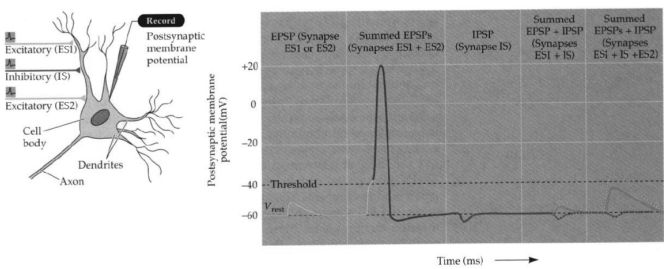

Figure 3.2: *Excitatory and inhibitory postsynaptic membrane potential [Purves et al.].*

synapse (IS). On the right, the change of the membrane potential upon synaptic activation is shown. An EPSP is produced by stimulation of either ES1 or ES2 (first fifth of the line in Figure 3.2). An even stronger EPSP is produced if both are stimulated at the same time (second fifth of the line). In contrast, when IS is activated, this will result in an IPSP (third fifth). Finally, the sum of EPSPs and IPSP is shown in the fourth and fifth fifths of the line [Purves et al.].

3.2 The Motor Cortex and Basal Ganglia

The brain is a complex system of many interconnected components tailored to process information from the environment. The motoric neural signals are processed at the base of the forebrain where the motor cortex and basal ganglia are located. Therefore these regions are the first place of investigation in order to gain insight and understanding of voluntary motoric neural signals. The primary role of the motor cortex is the control of the execution of movement, while the basal ganglia play a central role in the selection of voluntary movements. The basal ganglia consist of different parts, its input structure is called the striatum [Purves et al.].

The motor cortex and basal ganglia regions can be seen as part of a feed-back system (Figure 3.3) where the motor cortex gives input to the basal ganglia which in turn processes and filters the signal, before sending it to thalamus. Thalamus gathers the information then sends the signal back to te motor cortex. The processed and filtered signal is thereafter sent from the motor cortex to the brainstem and into the medulla oblongata, which is located in the lower half of the brainstem. The right hemisphere controls the left half of the body, while the left hemisphere controls the right half of the body; the medulla oblongata is the region where the signals cross over to the other side of the body. The neural impulses then pass from the medulla oblongata to the spinal cord which transmits the impulses to the muscles [Purves et al.].

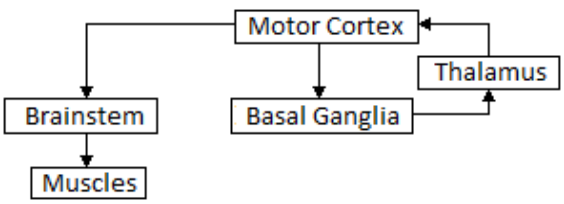

Figure 3.3: *Simplified block diagram of how the brain controls voluntary movements.*

The processing and filtering in the basal ganglia is initiated by the striatum which sends its signals through both a direct and an indirect pathway. Due to different combinations of exitatory and inhibitory synapses along these pathways, activation of the direct pathway excites the thalamus while activation of the indirect pathway inhibits the thalamus. If the indirect pathway is not working properly, there will be uncontrolled or involuntary movements, while there will be a slowness in the movements if the direct pathway is not working properly. It has

been suggested that the indirect pathway inhibits thalamus until the action has been properly planned and prepared and is ready to be sent through the direct pathway [Schmidt et al., 2013].

In general, all neurons in the brain have the same basic structure (see Chapter 3.1). However, there are structural and functional differences. The neurons that are of particular interest within the region of the motor cortex are interneurons (IN) and pyramidal neurons (PN's) [Purves et al.]. Interneuronal axons typically connect to neurons within the same structure. In contrast, PN's are so-called projection neurons, with axons extending to distant regions such as the striatum. In the striatum, 95% of the neurons are projection neurons of the type medium spiny neurons (MSN's). MSN's are inhibitory neurons and the main function is to regulate the neurons' activation in a region which can be outside the striatum. A recent research study shows that MSN's play a key role in encoding of locomotion and in environmental recognition. The remaining 5% are interneurons, where especially fast–spiking interneurons (FSI's) seem to play a critical role in the locomotion even though FSI's only represent a small portion of striatal neurons [Yamin et al., 2013]. The spike waveforms of different neuron types have distinct differences due to structural differences in the neurons. This is useful in the spike sorting process and by this, a specific neuron type can be determined (see Chapter 3.1).

3.3 Challenges of Brain Machine Interfaces

A brain machine interface (BMI) is a communication pathway between the brain and a device. The ultimate goal in this study is to find the neural signals that control locomotion which in the future can control such a device in real time. Therefore, it is important to understand the challenges involved in creating a BMI.

The first thing to consider is whether the data should be acquired via invasive means (i.e. brain surgery), or not. The most common invasive method is to implant one or more electrodes into the brain. The great advantage of this method is that it can directly record the activity of single neurons. Non-invasive methods (for instance electroencephalography (EEG) or functional magnetic resonance imaging (fMRI)) have the advantage of not requiring surgery, but the drawback of only being able to record the activity of large populations of neurons. As this study uses implanted electrodes this chapter will focus on the challenges of invasive methods.

An initial challenge is deciding where to implant the electrodes. Understanding the function of the different regions of the brain can help when making the decision. If the BMI receives signals from a brain region that is normally involved in the execution of movement, theoretically it should be easier to control intuitively than if it receives signals from a brain region that has nothing to do with movement. Examples of suitable brain regions are the motor cortex and basal ganglia, which have been mentioned earlier in the report (see Chapter 3.2). Much research has gone into understanding the nature of their involvement in movement but a great deal still remains unknown. Even after one or more regions have been chosen and the electrode has been implanted, it is still hard to know whether the electrodes

have been implanted correctly; they could very well miss the target. There is no reliable way to confirm their exact anatomical position in a living subject.

Another challenge is to develop a fully biocompatible device that is not rejected by the body, and can record neural signals with as little noise as possible. If the body rejects the electrode, the electrode will be covered with glia cells, which degenerate the recorded signal. With perfect biocompatibility the body would see the electrode as a part of itself and the signal would never degenerate.

Yet another challenge is to further develop a computational algorithm suited to process information and from the brain.

3.4 Ethics

Research using animals can give rise to strong feelings. However, the information which would otherwise not be obtained could potentially help thousands of people. The discussion of ethics tries to find an acceptable balance between the animals suffering and the value of the research. The animals should be able to live as good a life as possible. It is also imperative that animals should only be used in research that could not be done without them, and that no more animals than necessary are used. Animal experiments are only performed if it is approved by an ethics committee.

A widely accepted ethical framework is the three R:s of animal research: Replacement, reduction and refinement. Replacement seeks to find alternative research methods than experimentation using animals, like computer modelling or imaging. Reduction aims to use fewer animals for research by improving the research gained from each animal. Refinement seeks to improve the living condition of the research animals [CODEX].

Chapter 4
Problem Description

If a person sustains a spinal cord injury that results in complete paralysis, that person would be totally dependent on others for mobility. Having some freedom of movement restored would make a tremendous difference for this person's quality of life. What if, for example, this person was able to steer a wheelchair as if it would be its own body part?

When a spinal chord injury prevents the signals from the brain to reach the muscles in the body the result is paralysis. If those signals could be measured before being stopped at the injury in the spinal chord, these could be redirected to a wheelchair that could move forward when the brain tells the legs to walk. The present study, performed during six months, builds a small piece of the foundation for creating a wheelchair controlled directly by the brain.

The goal is to find the signals in the brain that control movements and teach a computer to predict the movement in order to foretell when locomotion is intended. The Basal ganglia and motor cortex are regions in the brain that are known to play an important role in voluntary movement and are therefore the target regions of this study. However, little is known about what the neural signals for movement look like in these regions.

This study uses neural data from the motor cortex and striatum of freely behaving rats and simultaneously recorded video data, in order to improve our understanding of how neural signals in these regions control locomotion. The first part of the project will focus on this while the second part of the project will focus on using the neural signals to predict when the rat intends to move. If the computer learns to successfully predict movement, then these results can be used as a foundation for future research devoted to developing a brain-controlled wheelchair.

Chapter 5
Methods

Planning and implementing a research project requires a lot of work and involves several important steps. First of all, an experimental design was developed by Neuronano Research Center (NRC) and suggested and approved by the Malmö/Lund ethics committee. Subsequently, surgery was performed on rats in order to implant electrodes so their neural activity could be recorded during the experiments. The rat's movement during the experiments was recorded by a monochrome video camera. After sacrificing the animal, histology (the study of brain tissue under the microscope) has occasionally been undertaken to validate the position of the electrodes. The recordings was then processed and analysed in the software Offline sorter and MATLAB. The neurons firing rate together with the movement data was analysed in a perievent time histogram (see Chapter 5.7.1) to visualise neurons' correlation of movement. The movement of the rat based on its neural activity is predicted by computer learning. Each step of the project is explained in detail below. The data used in this project is based on eight recordings from two adult female Sprauge Dawley rats (four recordings from each) conducted in 2010.

5.1 Experimental Setup

The experiments were performed in an open field environment. The open field setup consists of an enclosed square area, 75x75 cm. The rat was marked with color on rear, body and head, which will make it easier to track the animal when the video recording is later analysed, and placed to freely explore the environment while the video documented its behavior in parallel with the collection of neural data (see Chapter 5.5). Each experiment session was between six and ten hours long, usually overnight.

5.2 Multi-Electrodes

The multi-electrodes used in this project consist of 74 electrodes in total: 64 recording electrodes, eight reference electrodes and four stimulating electrodes. The electrodes are positioned in four equally large two-dimensional arrays in the regions of the striatum and motor cortex in the left and right hemispheres of the brain, which can be seen in Figure 5.1. Besides 16 recording electrodes, there

are also two reference electrodes and one stimulation electrode in each implanted region. Each recording electrode measures the changes in electrical potential as the neurons near the electrode fires action potentials. The recorded voltage from the selected reference electrodes is subtracted from the voltage from each recording electrodes. The function of the stimulating electrodes is to stimulate nearby neurons. The stimulating electrodes are however, not used in this project.

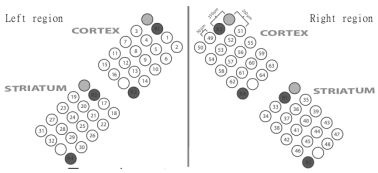

Figure 5.1: *The electrode layout shows where the electrodes are positioned in the left and right hemisphere of motor cortex and striatum. Light gray for stimulating electrodes, dark gray for reference electrodes and the remaining, white dots, are recording electrodes*[1].

The electrodes are made of tungsten, a metal with high signal-to-noise ratio (the average power ratio between neural signals and noise) and low impedance, where the impedance is the voltage divided by the current. Tungsten also has a high mechanical stiffness which makes it easier to puncture the brain tissue when the electrode is implanted. Lastly, it provides very good extracellular recordings. The drawback is a high noise level at low frequencies; this however, can be removed by a high pass filter. The electrode wires have a total diameter of 33 µm including a few µm thick polymer insulation. A small size of the electrode is desired as it will cause minimum damage to the neurons but it still needs to be thick enough to penetrate the tissue without bending. A smaller size of the electrode tip gives a lower current which gives a higher electrical resistance. A low electrical resistance is desired as it decreases thermal noise which in turn gives better signals from neural activity. The high impedance due to the small size of the electrode can be decreased through electroplating. This process uses an electrical current to form a metal coating on the electrodes. This will increase the surface area, which increases the current and therefore decreases the impedance.

To evaluate how good the electrodes are before implantation, an impedance test is sometimes performed. Impedance measurements are done with GAMRY Electrochemical Impedance Spectroscopy (EIS) software with a potentiostatic EIS setting mode (where the AC voltage is constant and the current can be quantified)[Gamry].

[1]Unpublished electrode layout picture, with permission from NRC for use in the report *Decoding Motor Commands in Cortico-Basal Ganglia Circuits for the Purpose of Controlling a Neuroprosthetic Device*

5.3 Surgical Procedures

During the surgery the rat is sedated with its breathing constantly monitored to ensure that it is neither about to wake up, nor too deeply sedated (which could stop its breathing). After the rat is unconscious it is placed in a stereotactic device, which puts its head into a fixed position. This is important in order to be able to set up a reliable frame of reference such as a bone landmark for the surgery (see Figure 5.2). As a first step of the surgery the skull is exposed by making a straight cut and pulling the skin to either side. Then the locations where the electrodes will be implanted are located with the help of an anatomical map, with the bregma as a reference point (see Figure 5.2). These locations are lightly marked with a drill. The markings are then carefully expanded until the holes go through the bone without penetrating the tissue below. The electrode array is positioned above the holes in exactly the right place and angle, and lowered carefully into the brain. The lowering is done either in small bursts (25 µm at a time) or slowly at a constant velocity (10 µm/s).

Once the electrodes have reached their intended depth, the areas of the brain that were exposed are covered with a protective gel. Then the electrode array is fastened to the skull using dental cement.

The entire surgery takes about five hours. After the operation the rat is allowed to rest for a week to fully recover.

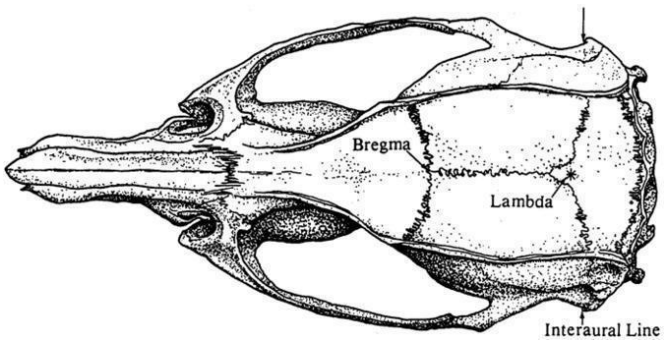

Figure 5.2: *The rat skull shows the bregma and the intersection of the four top skull bones. The bregma is used as a reference point during surgery in order to implant the electrode into the intended regions [Paxinos and Watson, 2007, 11]*[2].

[2]Reprinted from *The Rat Brain in Stereotaxic Coordinates*, Sixth Edition by George Paxinos and Charles Watson, Introduction, Page 11, Copyright 1982, with permission from Elsevier for use in the report *Decoding Motor Commands in Cortico-Basal Ganglia Circuits for the Purpose of Controlling a Neuroprosthetic Device*

5.4 Histology

Histology is the study of the microscopic anatomy of cells and tissues and is usually done by sectioning and staining. Histology is done mainly to confirm the position of the electrodes and to see what damage the region around the electrodes has suffered (mainly mechanical and inflammatory). In this study, a nucleic staining method called Nissl staining is used. Relevant regions of the brain are sectioned into roughly 25 µm thick slices and submerged with the dye cresyl violet that stains neurons, glia or other interesting cells. Regions such as the soma and dendrites are colored granular purple-blue, while other regions remain almost uncolored. Figure 5.3 shows an example of Nissl staining with cresyl violet dye. (a) is a histology with both hemispheres and (b) is a close-up of the left striatum were the two holes from the electrodes are seen in the middle of the picture.

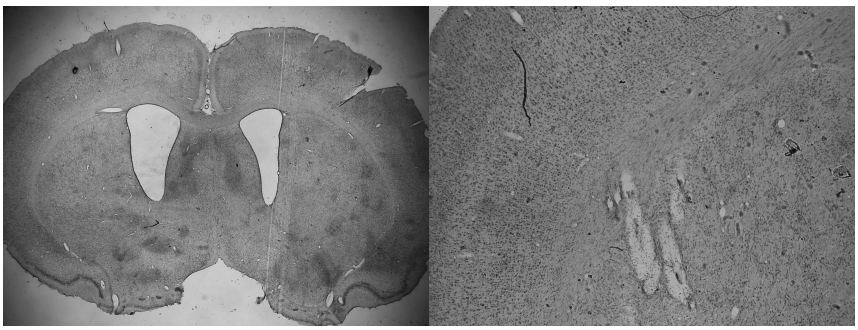

(a) **(b)**

Figure 5.3: *The Nissl staining with cresyl violet dye with pictures showing (a) both of the hemispheres and (b) a close-up of the left striatum [Integrative Neurophysiology][3].*

5.5 Data Acquisition

Neural spiking activity is recorded using multi–electrode arrays as described in Chapter 5.2. The signals are filtered with a bandpass filter with band width 600-9000 Hz and sampled at 32 kHz by a digital data acquisition system, Neuralynx, with Cheetah software version 5 (Neuralynx Inc.). The setup is presented in Figure 5.4. The headstage transforms the impedance and reduces the noise susceptibility. The rat's movement was recorded with a monochrome video camera (Dalsa Genie, 25 Hz) with a resolution of 640 x 480 pixels, and saved with Common Vision Blox software (Stemmer imaging Gmbh). A Master-8 pulse generator

[3]Unpublished Nissl staining pictures, with permission from NRC for use in the report *Decoding Motor Commands in Cortico-Basal Ganglia Circuits for the Purpose of Controlling a Neuroprosthetic Device*

(A.M.P.I. -Master-8) was connected to the camera and Neuralynx to synchronise their sampling.

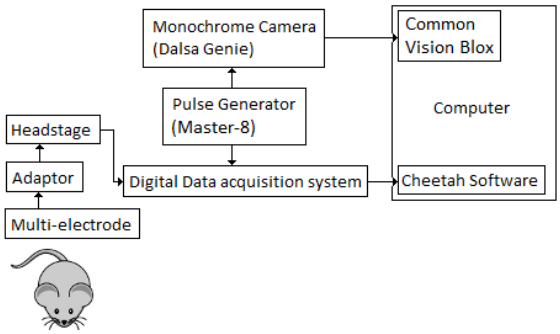

Figure 5.4: *Overview of the data acquisition.*

5.6 Data Preprocessing

The recorded data is preprocessed and refined for later analysis. The preprocessing consists of two main parts: spike sorting and video tracking. The spike sorting is where individual neurons are identified from the raw spike data containing all putative action potentials. The video tracking seeks to find where the rat is located in the open field at each time during the experiment and using that knowledge to determine when it moves. See Figure 5.5 for a general overview of how the data is processed in the project.

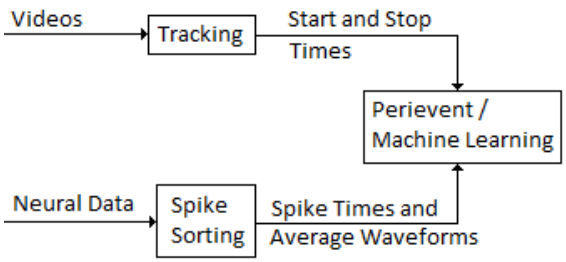

Figure 5.5: *Overview of the data input/output of the different parts of the project. The tracking uses the video data to determine when the rat starts or stops the movement. The spike sorting has the spike data as an input and separates actual spikes from noise, and also determines which neurons the spikes originate from. Both tracking and neural data are needed to do the perievent time histograms and the machine learning.*

5.6.1 Spike Sorting

A persistent challenge in spike sorting is the non-trivial separation of the data from the noise: On one the hand, as much of the noise as possible should be removed, but on the other, it is desirable to keep as many of the real spikes as possible. In order to do this sorting each spike's waveform is analysed. Features such as valley-, peak- and peak-valley width and principal components (see Figure 5.6) are common when separating spikes. To be noted is that the peak is pointing downwards and the valley is pointing upwards. This is due to the measurements which are taking place extracellular and not intracellular. The most useful features for spike sorting are

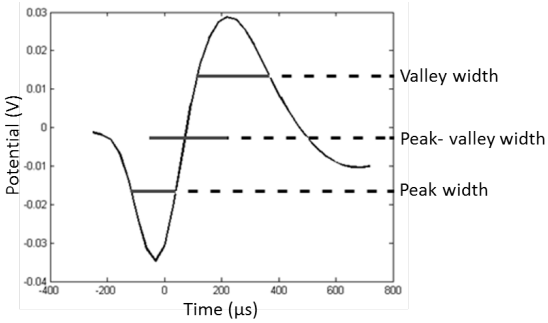

Figure 5.6: *Features of a spike's waveform which is measured extracellularly.*

usually the principal components. Principal component analysis (PCA) builds an n-dimensional space using the spikes waveforms, where n is the number of data points in each waveform. As can be seen in Figure 5.7, a number of waveforms are sampled and aligned to the start of each waveform (light gry and dark gray lines in (a)). A vector space (b) is then constructed by using each sampled time point (in this case t1 and t2) as a dimension. Each waveform can be represented as a point in the new space with the potential at t1 as its first coordinate and the potential at t2 as the second ([g1, g2] for the light gray line and [r1, r2] for the dark gray). If the waveforms are sampled at more times the potential at each time represents its coordinate in a dimension within the vector space. From this a third space is created (c) where each axis is a principal component that is a linear combination of the axes from (b). The first principal component (PC1) is the linear combination that accounts for most of the variance between the points in (b). The second principal component (PC2) is orthogonal to the first principal component, and accounts for the second highest variance. In this example PC1 would be along the line that connects the two points, while PC2 would be zero for both as all the variance has already been accunted for. The linear combination for PC1 and PC2 would be:

$$PC1 = \frac{t_1 - r_1}{2(g_1 - r_1)} + \frac{t_2 - r_2}{2(g_2 - r_2)} \tag{5.1}$$

$$PC2 = \frac{t_1 - r_1}{2(g_1 - r_1)} - \frac{t_2 - r_2}{2(g_2 - r_2)} \tag{5.2}$$

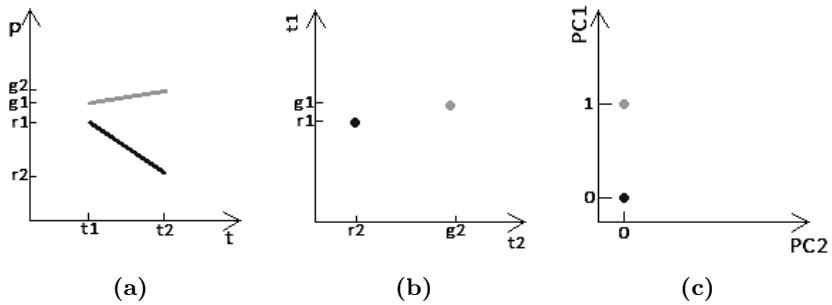

Figure 5.7: *Example of how principal component analysis works. (a) The dark and light gray lines are sampled waveforms at their respective sample points (t1 and t2). (b) Is a vector space, with the amplitude at the sample points as the dimensions, where waveforms is represented as a point. (c) Is a vector space where the dimensions are orthogonal linear combinations of (b).*

The first few principal components account for the highest variances between waveforms and are therefore, very useful when spike sorting as each neuron has its own characteristic waveform. The different waveform types make it possible to classify each SU from striatum and motor cortex. This classification was done through fuzzy k-means clustering. This method calculates the probability to belong to the different types for each neuron based on how close their peak widths, valley widths and peak-to-valley widths are to the known mean values for each type. The neuron will be classified as a certain neuron type if the probability for belonging to that type is above a given level.

The two main objectives in spike sorting are to separate the falsely detected action potentials (noise) from the correctly detected action potentials (spikes), and to identify the individual neurons that fired the spikes. The action potentials are sorted, using the program Offline Sorter, into unit clusters. These clusters can be identified to be noise or to come from one neuron, called single unit (SU), or several neurons, called multi units (MU). In this study, the spikes have mainly been manually sorted. An overview of the software's functionality can be seen in Figure 5.8. An identified unit is marked with white while the noise is gray. In (a) each spike's waveform is plotted with voltage on the y-axis and time on the x-axis. What the waveform looks like depend on the neuron [Purves et al.]. In (b) each unit's mean waveform is plotted (top) as well as a histogram of its inter-spike intervals (ISI) (bottom), that is the time between spikes. The percentage in red shows the percentage of the inter-spike intervals that are shorter than 1.6 ms. This number is chosen as no neuron is believed to have such a short refractory period. A high inter-spike interval fraction either means there is a lot of noise or that the grouped spikes originate from more than one neuron. If the percentage is below

0.1% (shown in the upper areas of Figure 5.8(b)) then the unit is classified as a SU. It is classified as a MU if the percentage is above 0.1%. It is generally good to keep this percentage as low as possible. In (c) the spikes are plotted in the current feature space, each dot represents a spike. When sorting one generally has to browse through a number of features (characteristics) to find a clear separation of a neuron's spikes. If the signal is very good the spikes from a neuron will be clearly separated from the noise and other neurons.

Another interesting feature of the neuron is its autocorrelation. While the ISI is the time between two spikes, the autocorrelation takes into account the time to all other spikes at once. It is a good way to see if the neuron has a repeating firing pattern.

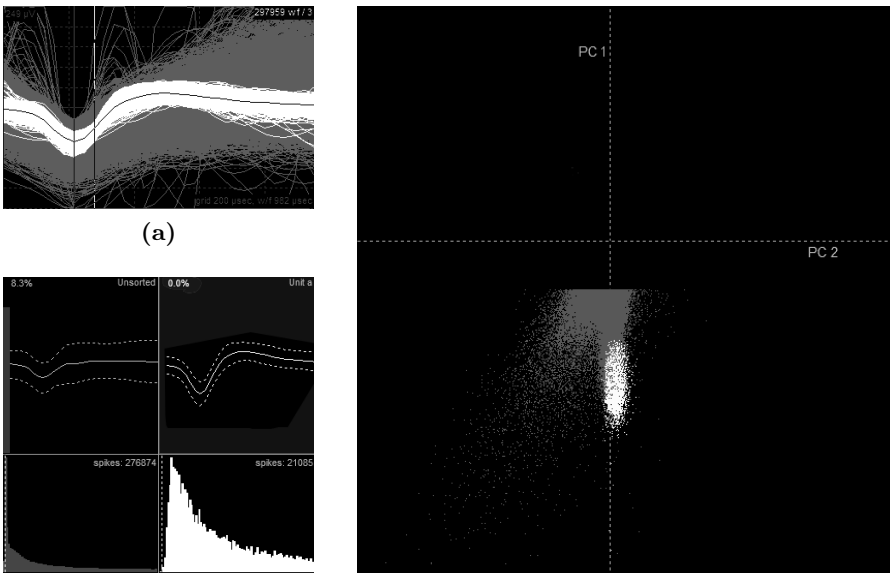

Figure 5.8: *A typical view of spike sorting in Offline Sorter. A neuron that has been sorted has its spikes shown in white and all unsorted spikes are in gray. (a) Shows the waveforms of all spikes from the selected electrode. (b) Shows the mean and standard deviation of the different groupings of spikes (top) and the spikes' ISI (bottom). (c) Shows each spike's first two principal components.*

5.6.2 Video Tracking

The goal of video tracking is to find out at what times the animal shows a behavior that is relevant, in this case when the rat moves.

Because it was not realistic to go through the video manually and mark when the rat moves, the tracking had to be done automatically. First, the rat's position

at each frame had to be found. This was done using the tracking toolbox Open Field Tracking GUI, developed at NRC (see Figure 5.9). It does this by first taking the mean of a portion of the frames in the video to find the background (because the rat moves it will not be visible after the averaging). It then identifies a region of interest (ROI) that contains the rat in each frame by finding the area that differs most from the background, which in these experiments are the three markings on rear, body and head (see Chapter 5.1).

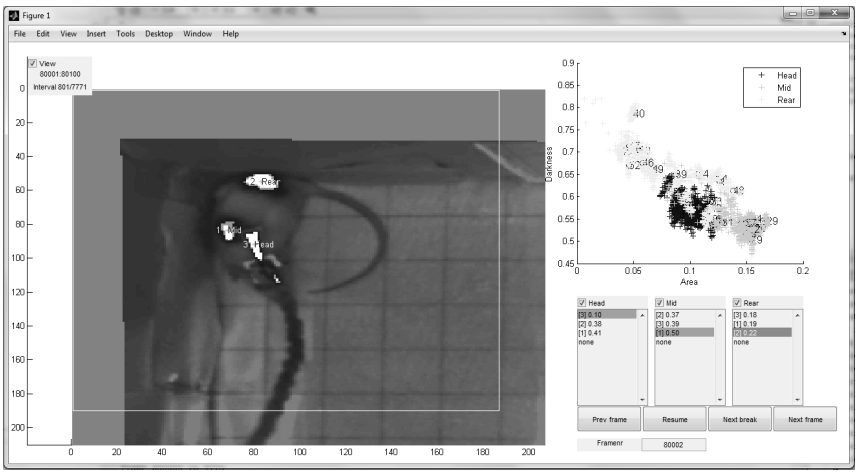

Figure 5.9: *The OpenFieldTrackingGUI (developed at NRC and implemented in* MATLAB*) was used to track the rat in the open field. The rat has markings on the head, body and rear to help with the tracking. The OpenFieldTrackingGUI highlights the markings it has found in the first video frame (left) and the user determines which marking belongs to what part (bottom right). The program then proceeds automatically through the recording until it has finished all video frames or looses track of some of the markings, in which case the user will be questioned again.*

When the rat's position is known the velocity can be calculated by the distance the rat moves between frames. The velocity was limited to a binary movement on/off-vector, which was used to predict the movement bouts. Each sufficiently long interval of movement that was preceded by a certain time of stillness was classified as a movement bout. The threshold and length of movement/stillness was tweaked manually to optimize the accuracy of the prediction. However, not all bouts where captured with this method which is why a second method; fail-safe, was implemented. The fail-safe noted each time the animal passed between quadrants of the open field. Because the rat prefers to spend its inactive time close to a corner the moment it passes over a middle line is almost exclusively during a

movement bout. With these two methods the work in finding the movement bouts was kept to a minimum, although the timing still had to be fine tuned manually.

The recorded movement bouts are checked manually using BehaviourGUI, a MATLAB toolbox developed by NRC (see Figure 5.10). BehaviourGUI allows the synchronisation of different time periods, videos and events. It allows fast forwarding of the video in one window to predefined event times (start and stop), while showing the tracked velocity for the same time in a different window. Here start and stop times are manually fine-tuned and new bouts can be added if the first detection failed to find them.

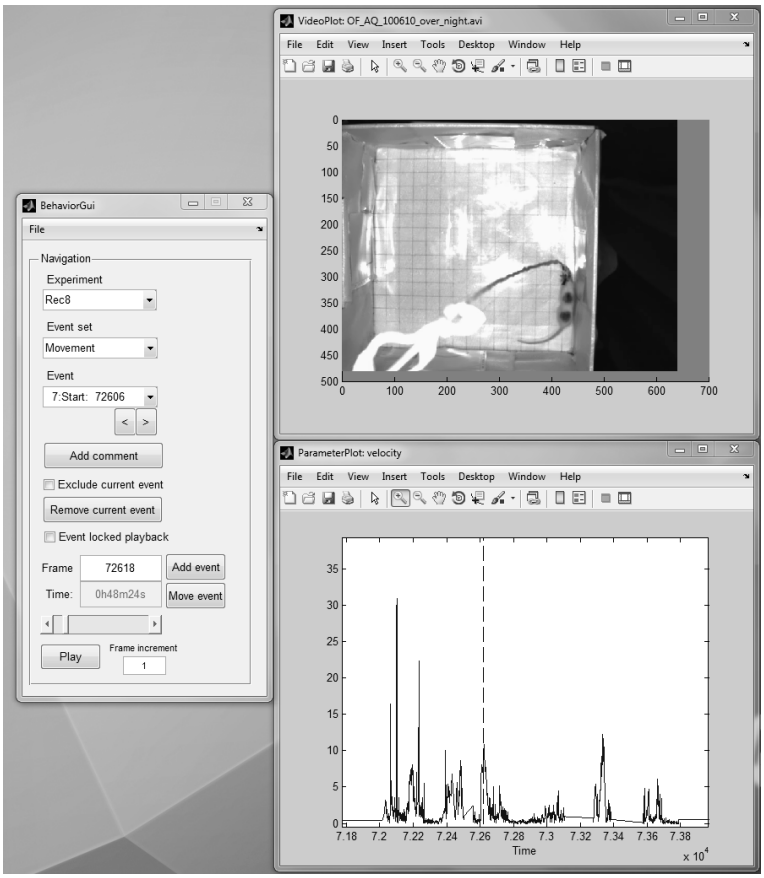

Figure 5.10: *The BehaviourGUI toolbox allows data to be synchronised so several data sets (such as a video recording and computed velocity) easily can be analysed simultaneously. This is of great help when trying to find when the rat is moving.*

5.7 Data Analysis

5.7.1 Perievent Time Histogram

Perievent time histograms represent a means to visualise whether the neurons firing of action potentials (firing rate) systematically changes at certain re-occurring events, for instance start and stop movements of the rat. The perievent time histogram shows a summation of the neuron's activity during a number of events (see Figure 5.11). First a number of events are selected (a), in this project such events would be movement bouts, or when the rat starts and stops moving. When the time points for the events have been found, the neuron's firing rate around these times is extracted (boxes 1-6). The firing rate is calculated by dividing the time into bins, counting the number of spikes in each bin and dividing that number by the size of the time bin. These firing rates are aligned to the start time of the events (b) and summed to create a perievent time histogram (c). To

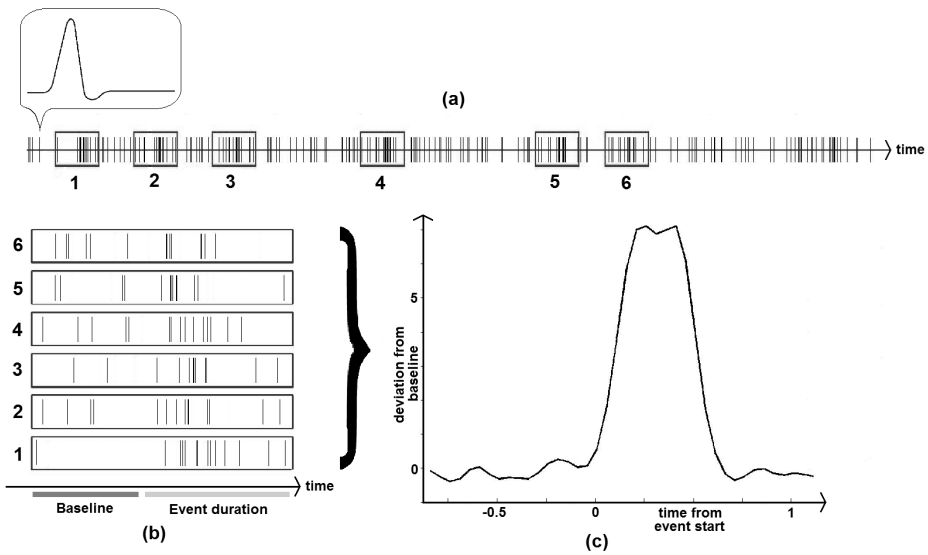

Figure 5.11: *A perievent time histogram shows a neuron activity during a certain type of event.*

compare the activity during the event to the normal activity of the neuron, this sum is normalised to a baseline by subtracting the mean and dividing by the standard deviation of the baseline. The baseline is usually a time period prior to the event when the neuron's activity is assumed to be normal (unaffected by the event). If the neuron's firing pattern changes during these times there will be a clear modulation in the perievent time histogram. The higher the amplitude is near an event the higher the possibility is that the peak is due to the event. The computation of the perievent time histograms were made in MATLAB and the flowchart of the code can be seen in Figure 5.12. The neurons was split into

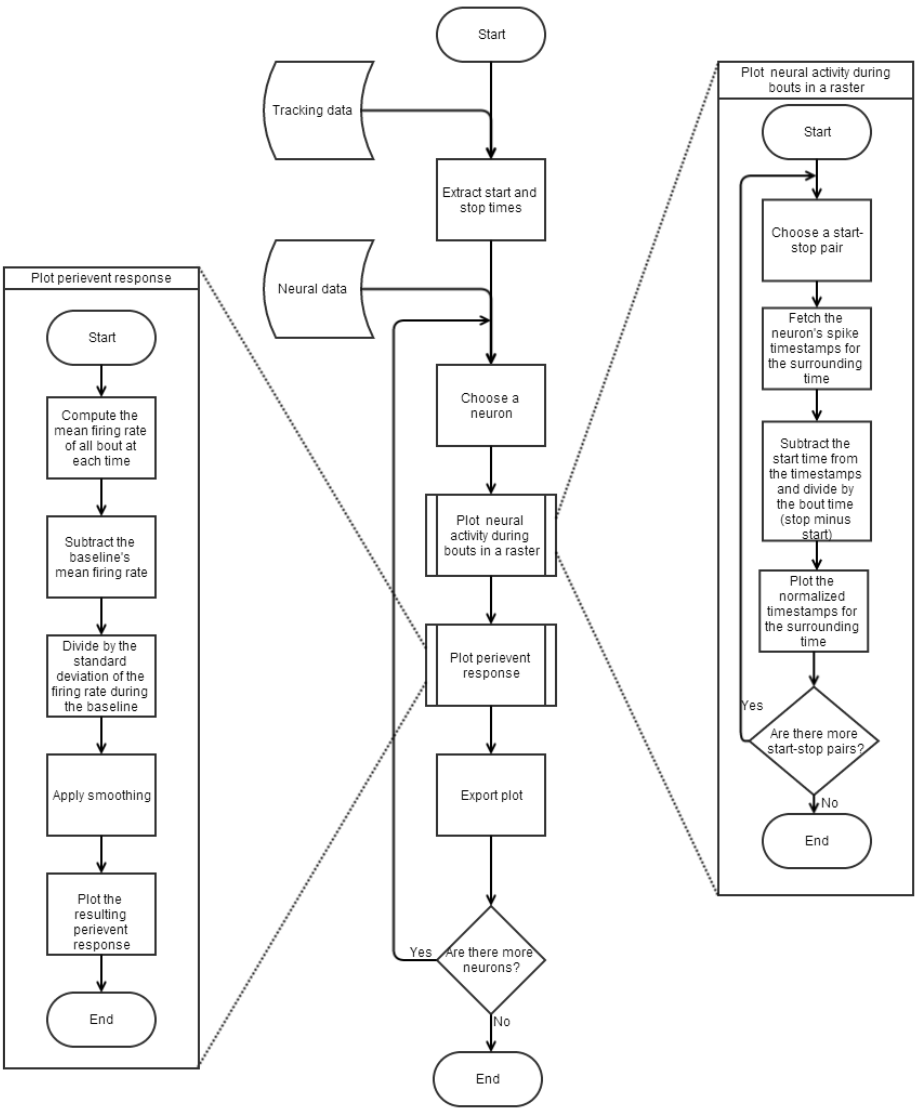

Figure 5.12: *Flowchart for computing the perievent time histograms.*

three groups based on their perievent response. If the perievent shows a clear modulation around the event times it is said to be correlated to the event. No clear modulation is seen it is said to be uncorrelated and if there are only a few sporadic spikes the neuron is said to be untrustworthy due to poor spike sorting. This grouping is done by visually inspecting the perievent time histograms.

Before proceeding to the computer learning, all movement data from the video tracking was downsampled by a factor of three, so the resulting time resolution was 3*1/25Hz = 120 ms.

5.7.2 Computer Learning

The computer learning is the final stage of the data analysis. The goal is to predict when the rat is moving based on its neural activity. The neurons have a specific firing rate, which is the average number of spikes per time interval and used in the general linear model [Carmena et al., 2003]:

$$Y = XA + E, \tag{5.3}$$

where Y is a binary $Nx1$ vector of observations at times $t_1, \cdots, t_N$ (in this case it is 1 if the rat is moving and 0 if it is still), X is an NxM matrix where each column represents the firing rate of a neuron during an interval (bin) with a certain bin size at a specific time (lag) from the observation (see Figure 5.13). Depending on the chosen bin size and number of lags, the model extends differently long into the past from each observation time. M is the number of neurons multiplied by the number of time lags plus one for a general offset. A $(Mx1)$ represents the weight (importance) of each column in X and E $(Nx1)$ is the errors (difference between the observed Y and the predicted XA).

$$\begin{bmatrix} y_1 \\ y_2 \\ \vdots \\ y_N \end{bmatrix} = \begin{bmatrix} x_{1,1} & x_{1,2} & \cdots & x_{1,M} \\ x_{2,1} & x_{2,2} & \cdots & x_{2,M} \\ \vdots & \vdots & \ddots & \vdots \\ x_{N,1} & x_{N,2} & \cdots & x_{N,M} \end{bmatrix} \begin{bmatrix} a_1 \\ a_2 \\ \vdots \\ a_M \end{bmatrix} + \begin{bmatrix} e_1 \\ e_2 \\ \vdots \\ e_N \end{bmatrix} \tag{5.4}$$

This model tries to make XA as close as possible to the observed values by taking the sum of the firing rates at each row in X multiplied by a constant in A for each column.

The computer learning is divided into two phases; training and prediction. In the training phase the best estimation of A is found by solving the least square regression model (Equation 5.3) for A

$$A = (X^T X)^{-1} X^T Y \tag{5.5}$$

Both X and Y need to be known in this phase and the more observations there are the better the estimated A will be, provided that the neurons in X are correlated to the movement.

Once A is known it is possible to move on to the prediction phase. In this phase Y is unknown and will be predicted by $Y = XA$. Then the prediction is evaluated by its receiver operating characteristic (see the explanation of receiver operating characteristic below).

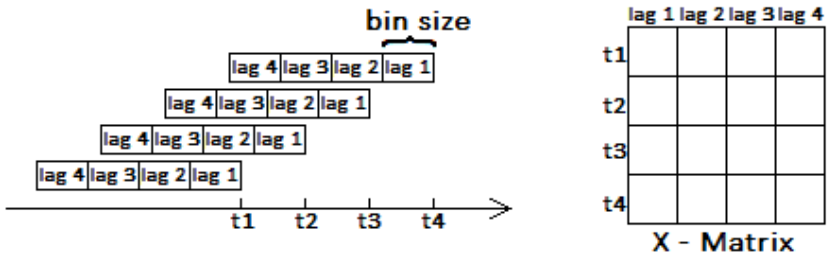

Figure 5.13: *The build-up of the X matrix. Each row represents one point in time and its columns contain the data to predict the behavior at that time. The data for each row is sampled in a number of bins from the time of the observation and back. To the left it can be seen where in time those bins could be for a certain configuration of bin size and number of lags. The right side shows where in the X matrix the firing rate in the bins should go.*

Five-fold cross validation was used in this project, meaning the data was split into five sections. Four was used for training and the last for evaluation. The sections used for testing and training was rotated five times in order to test the entire data set. A flowchart of the code for the machine learning is showed in Figure 5.15 at the end of the chapter.

Receiver Operating Characteristic

When binary data is used for training it is desirable to get a binary prediction. The easiest way to achieve this is to threshold the prediction (the rat is assumed to move when the prediction certainty is above the threshold). To decide a suitable threshold the Receiver Operating Characteristics (ROC) can be used.

There is seldom a threshold that gives a perfect prediction, therefore a compromise must be made. If it is important to predict all times when the rat is moving (true positive) the threshold should be low, but then it will also predict it is moving sometimes when it is actually still (false positive). If it is important to have few false alarms or predict all times when it is still (true negative) the threshold should be set high, but then it will sometimes predict the rat to be still even though it is moving (false negative). In other words the, value will be true positive if both real value and the predicted value is positive, false positive if only the prediction is positive, true negative if both are negative and false negative if only the predicted value is negative. The outcome false positive and true negative can be explained with the same concept in Table 5.1 [Fawcett, 2006].

Predicted value	Real value: Positive	Real value: Negative
Positive	True Positive	False Positive
Negative	False Negative	True Negative

Table 5.1: *The table summarises the four outcomes when a predicted value is true/false compared to the real value. The real and predicted values are either positive or negative. If the predicted and real value are the same, then the predicted value is true (true positive or true negative), and if these values differ, then the predicted value is false (false positive or false negative).*

A ROC curve can be used to get a sense of the balance between these parameters so a suitable threshold level can be set. The ROC curve is therefore built up by the true positive rate (TPR) as a function of the false positive rate (FPR). The TPR denotes the number of true positives (TP) that are predicted out of all real positive values (P) [Fawcett, 2006]. The real positive values can be written as a function of TP and false negatives (FN).

$$TPR = \frac{TP}{P} = \frac{TP}{TP + FN} \tag{5.6}$$

FPR shows how many of the negative values (N) are falsely predicted as positive, where N can be written as a function of false positives (FP) and TN.

$$FPR = \frac{FP}{N} = \frac{FP}{FP + TN} \tag{5.7}$$

A larger area under the ROC curve means a better prediction which can be seen in Figure 5.14. A ROC curve with an area of 1.0 a.u. would mean a perfect prediction and an area of 0.5 a.u. would mean a prediction at chance level [Fawcett, 2006].

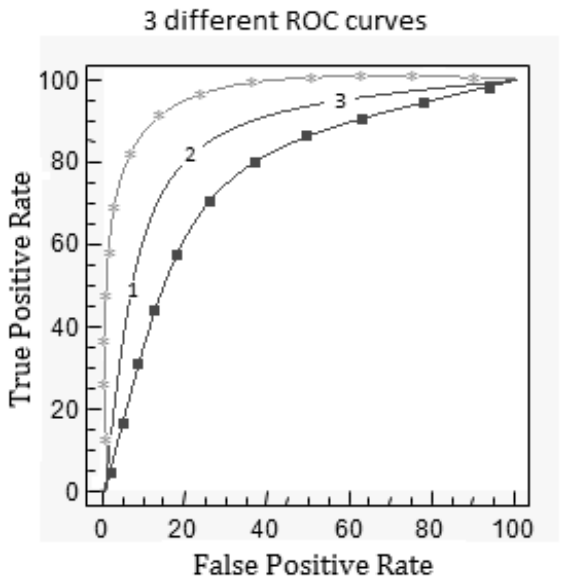

Figure 5.14: *Three hypothetical ROC curves represent the precision, where the light gray curve has the best precision of the three due to its large area underneath the curve. The middle line has three positions marked. Position 1 gives a stricter threshold of movement prediction (stricter false positive rate) than position 2 and 3.*

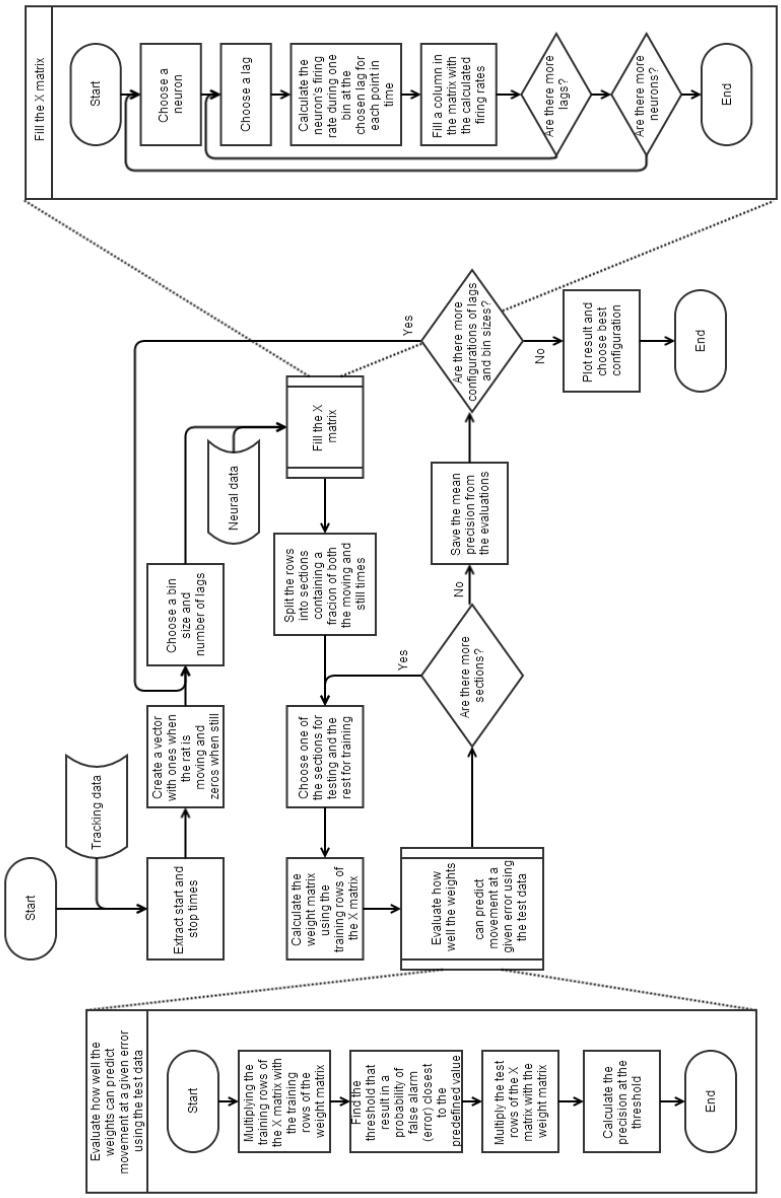

Figure 5.15: *Flowchart for using a linear model for prediction of movement.*

Chapter 6
Results

This chapter presents the results from the data preprocessing, with spike sorting and video tracking, data analysis with perievent time histograms and computer learning. Four experiments each from rat A (experiments A1-A4) and rat B (experiments B1-B4) have been analysed.

6.1 Data Preprocessing

6.1.1 Spike Sorting

A total of 105 neurons were sorted across the experiments of which 89 were identified as SU's and 16 as MU's. The neuron types were classified into four different categories depending on the features of waveforms (seen in Figure 6.1). Some of the structural features and functional differences of the neuron type clusters are shown in Figure 6.2. (a) and (c) are from the motor cortex and (b) and (d) are from the striatum. The two figures above show the peak to valley length as a function of peak width and the two figures below show the peak to valley width as a function of valley width. The values of specific waveform features (peak width, valley width and peak-to-valley time) together with standard deviation are written in Table 6.1. From these features, neuron types were classified as follows: 50 PN's and 7 IN's were found in the motor cortex. 27 MSN's and 11 FSI's were found in the striatum. A total of 10 neurons remain unidentified (UIN) (See Table 6.2).

Structure	Cell type	Peak width (µs)	Valley width (µs)	Peak-to-valley time (µs)
Striatum	MSN	155 ± 13	401 ± 56	299 ± 27
Striatum	FSI	121 ± 23	137 ± 47	158 ± 36
Striatum	UIN	159 ± 0	235 ± 0	252 ± 0
Motor cortex	PN	162 ± 13	432 ± 31	316 ± 25
Motor cortex	IN	143 ± 33	193 ± 77	210 ± 59
Motor cortex	UIN	156 ± 11	363 ± 18	245 ± 60

Table 6.1: *A table of features from MSN, FSI, PN, IN and UIN in the motor cortex and striatum.*

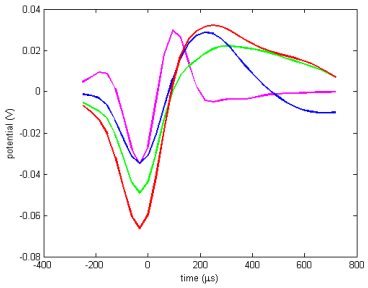

Figure 6.1: *Waveforms from the neuron types PN (green), IN (blue), MSN (red) and FSI (magenta).*

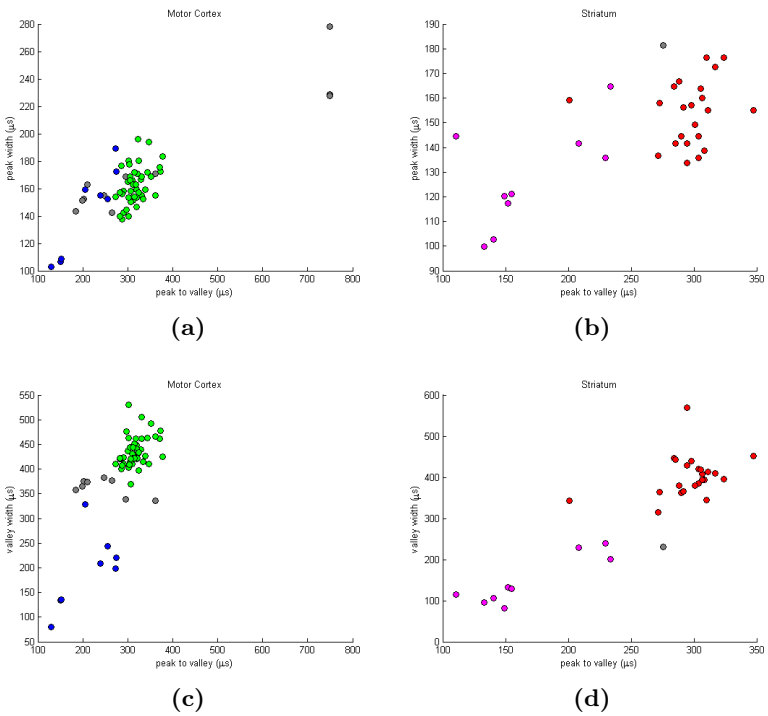

Figure 6.2: *Classification of putative neuron types for the motor cortex ((a) and (c)) and the striatum ((b) and (d)). For the motor cortex: PN (green), IN (blue) and UIN (gray). For the striatum: MSN (red), FSI (magenta) and UIN (gray).*

	Motor cortex			Striatum		
Experiment	PN	IN	UIN	MSN	FSI	UIN
A1	8	1	3	5	0	0
A2	9	1	2	6	1	0
A3	10	2	0	1	4	0
A4	6	0	0	0	3	1
B1	6	0	0	8	0	0
B2	2	0	2	2	0	0
B3	6	3	2	1	1	0
B4	3	0	0	4	2	0
Total	50	7	9	27	11	1

Table 6.2: *Number of neurons, with type classification depending on the waveform, found in respective brain region from each experiment. The classification were made on the neuron types PN, IN, FSI and MSN. Other neurons which could not be classified was named UIN.*

6.1.2 Video tracking

Tracking from video recordings of B1 shows that the rat mostly kept going near the sides. An example of this is shown in Figure 6.3 where dark gray is where the rat moves and light gray is where it is still. A specific threshold for when the rat was moving was set to 1.25 pixels/frame (see Figure 6.4). The tracking could not always decide which body part was which, jumping back and forth between them, resulting in huge spikes in the calculated velocity (see Figure 6.5a) (a). More accurate, semi-manual, tracking was made for experiment B1 (see Figure 6.5a(b)). Using this tracking would require less manual fine-tuning and the fail-safe would be unnecessary, but the semi-manual tracking is so time-consuming that the less accurate tracking is more time effective. Tracked positions (from the marked head point) and the respective velocity bouts from experiment B1 are shown in Figure 6.7 and 6.6. The axes for time, position, and velocity are not marked in the figures. This information is, however, not important in these cases as these are used to compare the different bouts to each other.

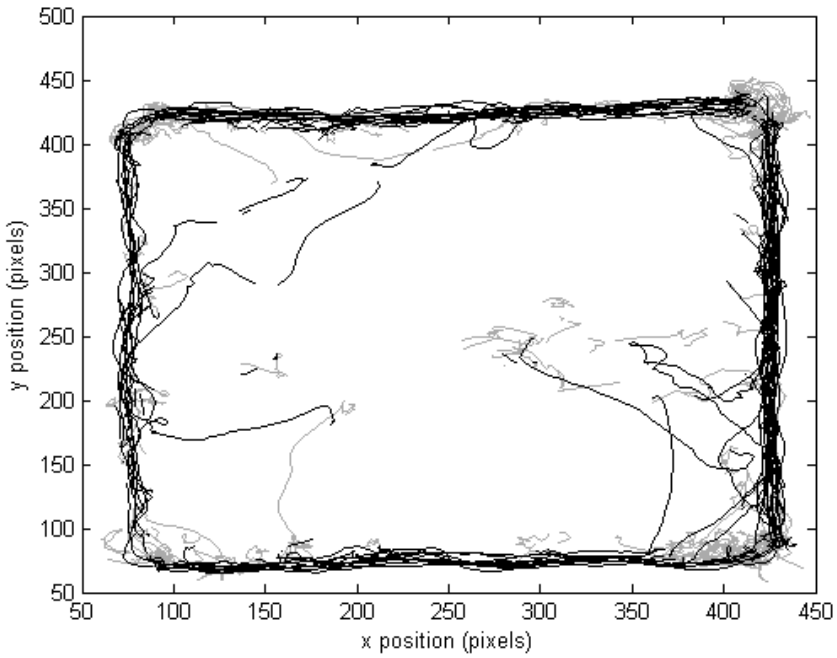

Figure 6.3: *Position of the rat during the whole experiment B1. The dark gray lines show where it is moving and the light gray lines show where it is still.*

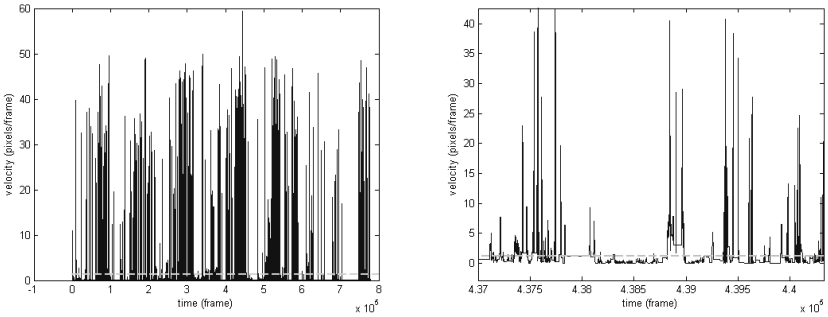

(a) **(b)**

Figure 6.4: *Threshold for when velocity is detected where (b) is a zoom in of (a).*

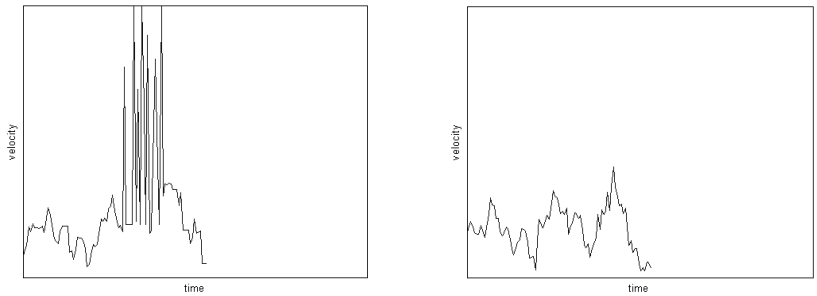

(a) **(b)**

Figure 6.5: *Velocity of the rat tracked (a) automatically and (b) with semi-manual tracking.*

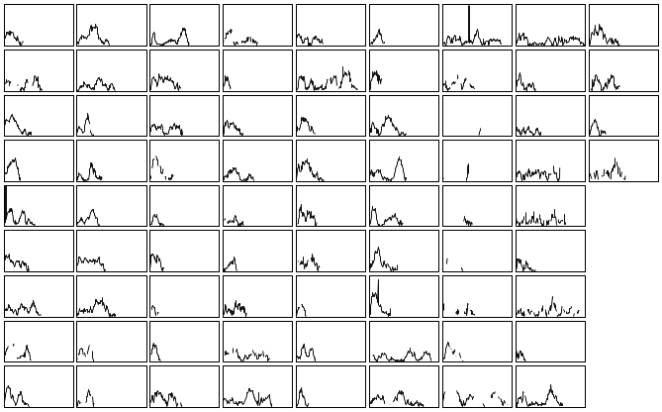

Figure 6.6: *Tracked velocity (from the point marked on the head) over time of the rat during movement bouts. The axes values have been left out as the focus is the shape of the bouts in relation to each other.*

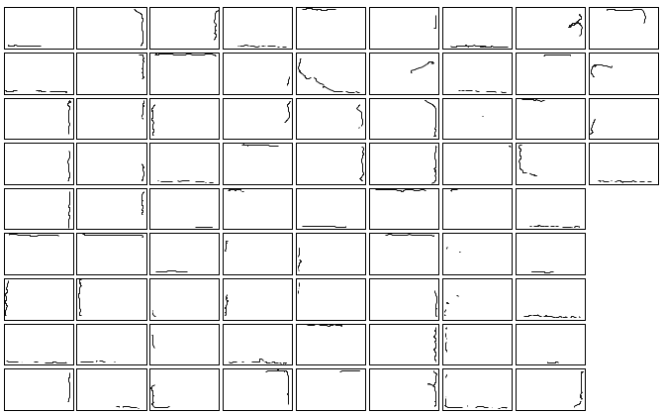

Figure 6.7: *Tracked position (from the point marked on the head) of the rat during movement bouts.*

A total of 536 movement bouts was tracked across the experiments, distributed according to Table 6.3. Experiment B4 was excluded from the project because only eight movement bouts was found for that experiment (not included in the analysis).

Experiment	Bouts	Duration (s)	Covered Distance (cm)	Velocity (cm/s)
A1	35	2.3 ± 0.9	19.5 ± 12.8	8.5 ± 4.3
A2	38	1.9 ± 0.9	16.5 ± 12.7	8.4 ± 8.9
A3	66	1.9 ± 0.8	22.8 ± 14.0	11.9 ± 5.2
A4	48	2.1 ± 1.1	19.9 ± 12.8	9.9 ± 5.3
B1	76	3.0 ± 1.5	26.2 ± 16.8	9.1 ± 4.5
B2	113	2.5 ± 1.4	21.1 ± 14.9	8.6 ± 4.1
B3	160	2.1 ± 0.8	26.2 ± 14.8	12.6 ± 5.7
Total	536	2.3 ± 1.2	23.0 ± 14.8	10.4 ± 5.3

Table 6.3: *Number of movement bouts with the mean and standard deviation of its duration, covered distance and velocity.*

6.2 Data Analysis

6.2.1 Perievent Time Histogram

A visual inspection of the 96 perievent time histograms shows that: 20 of 96 neurons seem to be correlated to movement; 45 neurons seem to be uncorrelated to movement; and 31 neurons were discarded because no analysis can be made of these due to too few spikes. The neurons are distributed according to Table 6.4. Experiment B4 is not included in the table due to too few movement bouts.

Experiment	Correlated	Uncorrelated	Discarded
A1	5	7	5
A2	1	10	8
A3	2	12	3
A4	3	5	2
B1	4	6	4
B2	1	3	2
B3	4	2	7
Total	20	45	31

Table 6.4: *Number of neurons which are correlated and uncorrelated to movements and discarded.*

There exist results from perievent time histograms of neurons that are visually correlated and uncorrelated to movement or discarded. The histograms show an alignment from start (light gray dashed line) to stop (dark gray dashed line). As the perievent time histograms are aligned to both start and stop the x-axis show the fraction start to stop rather than time. Examples of perievent time histograms for correlated, uncorrelated and discarded neurons can be seen in Figures 6.8, 6.9 and 6.10 respectively. Information of the different boxes in the perievent figures are explained in Chapter 5.6.1 and 5.7.1. The information box "Electrode layout"

in the figures of perievent time histograms is not used but if it would be used then the layout would be similar to what is shown in Figure 5.1. All perievent time histograms can be found among the complementary pictures [Moa Svensson and Joel Sjöbom, 2014].

When the correlation of the neurons was divided based on the neuron type, it was found there were significantly more correlation in the striatum than motor cortex (Z-test, $p < 0.05$, see Table 6.5).

Region	Type	Correlated	Uncorrelated	Discarded
Striatum	MSN	9	9	5
Striatum	FSI	1	5	2
Striatum	UIN	2	0	0
Motor Cortex	PN	5	24	15
Motor Cortex	IN	0	2	6
Motor Cortex	UIN	3	5	3

Table 6.5: *Number of correlated, uncorrelated and discarded neurons based on neuron type.*

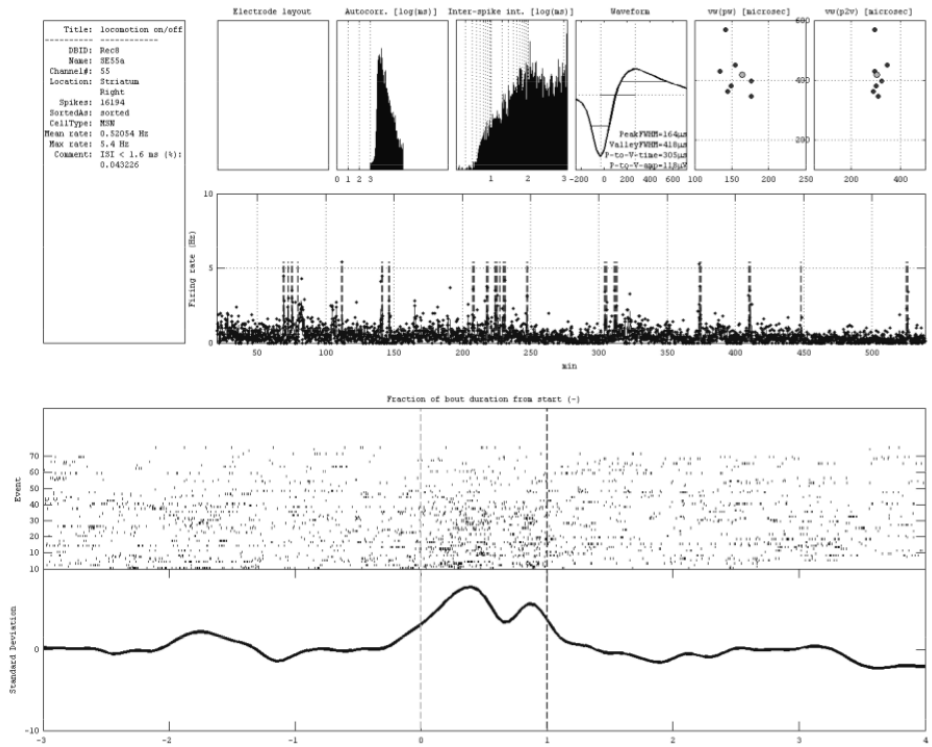

Figure 6.8: *Example of a perievent time histogram of a neuron that is clearly correlated to movement (upon visual inspection). The histogram shows an alignment from start (light gray line) to stop (dark gray line).*

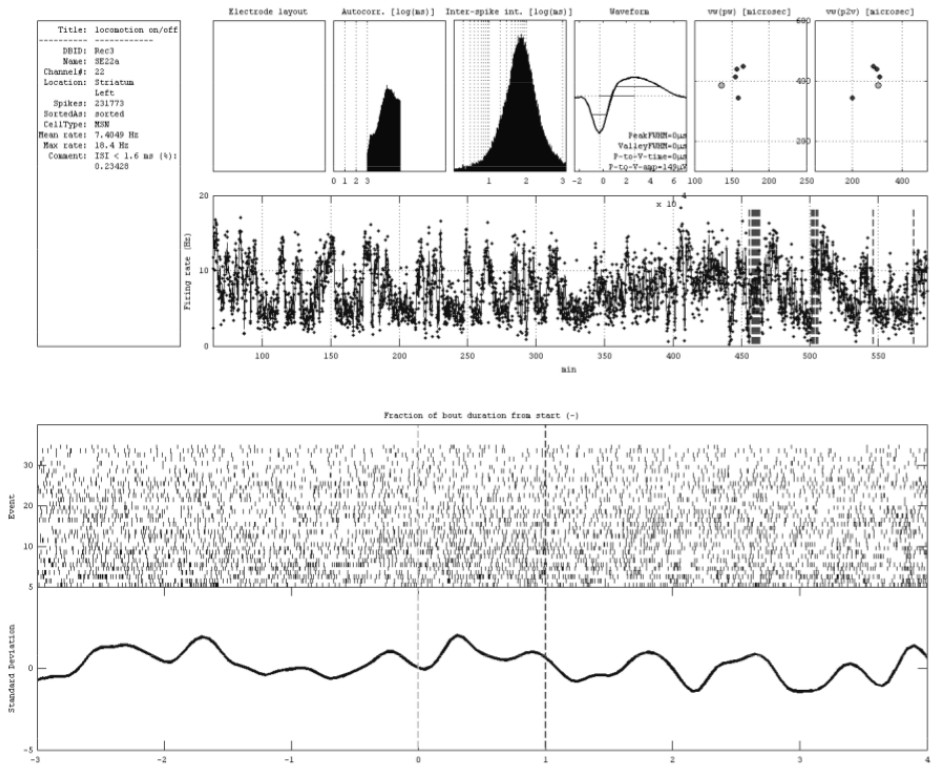

Figure 6.9: *Example of a perievent time histogram of a neuron that is not correlated to movement (upon visual inspection). The histogram shows an alignment from start (light gray line) to stop (dark gray line).*

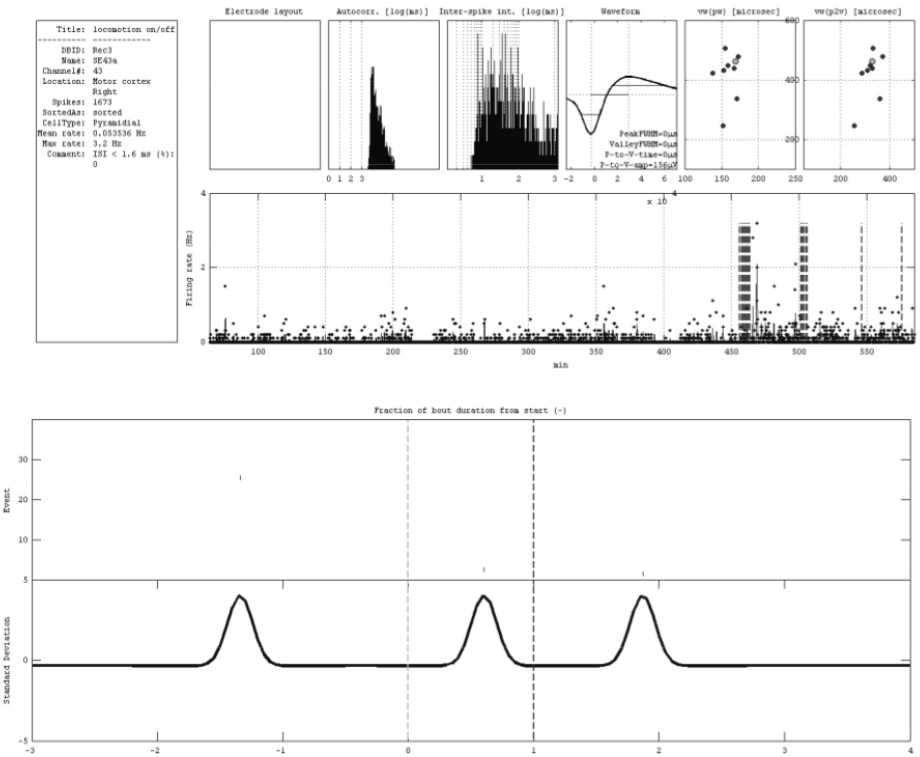

Figure 6.10: *Example of a perievent time histogram of a neuron that is discarded (upon visual inspection). The histogram shows an alignment from start (light gray line) to stop (dark gray line).*

6.2.2 Computer Learning

The effect of varying the number and size of time bins used in the general linear model has been systematically evaluated. Figures 6.11. (a)-(c) show the result of the computer learning from experiment A3, and the other computer learning results can be found among the complementary figures [Moa Svensson and Joel Sjöbom, 2014]. (a) shows the predictions of $1-FPR$ (left column) and TPR (right column) for the training data set (top) and test data set (bottom). (b) presents the area under ROC curves for training (left column) and test session (right column). In (a) and (b) the bin size is changed across the y-axis and the number of lags are changed across the x-axis. The brightness of each square represents how good the prediction is. (c) gives the time scale (bin size multiplied by number of lags) for each square in (a) and (b).

Figure 6.12a shows the prediction of movement for the data set from experiment A3 when the bin size is set to be 0.3 s and number of lags are five. Figures of prediction of movement from other experiments can be found in the complementary figures [Moa Svensson and Joel Sjöbom, 2014]. The black line in Figure 6.12a is the predicted movement from the video tracking data. The prediction is binary, were 1 indicates it is moving and 0 indicates it is not moving. The gray line is the predicted movement trained by computer learning. The threshold for movement is in (b) set above 0.5. The gray line is increased to a value slightly above 0 and slightly underneath 1 to easier evaluate the prediction of movement from both the computer learning and video tracking.

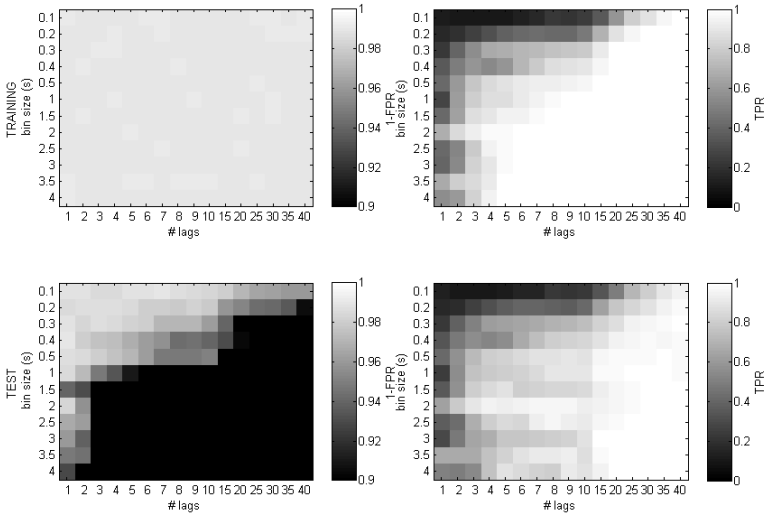

(a)

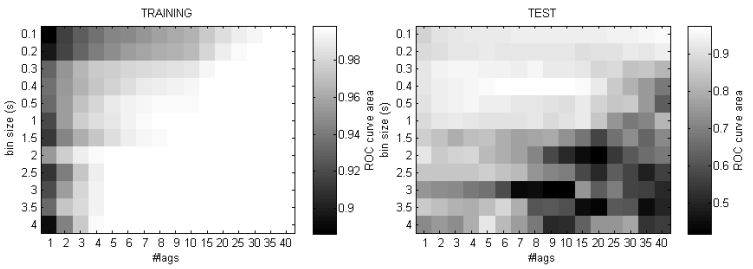

(b)

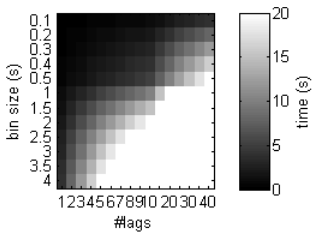

(c)

Figure 6.11: *(a) Evaluation of different configurations of lags and bin sizes in the general linear model. $1 - FPR$ in the left column and TPR in the right column. Upper row: training section, lower row: test section. (b) Area under ROC curves for training (left column) and test section (right column). (c) How long the general linear model extends into the past from each observation time for each combination of bin size and number of lags.*

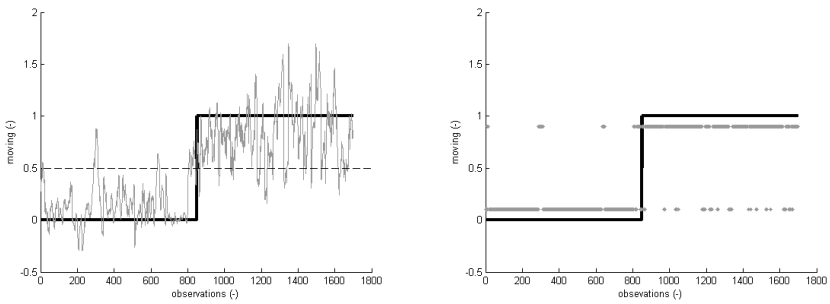

(a) **(b)**

Figure 6.12: *Predicted movement (gray line) and actual movement (black line). (a) shows the likelihood for movement according to the computer learning while (b) shows the prediction after a threshold at 0.5 has been applied.*

Chapter 7
Discussion

7.1 Regarding procedures during the project

Experiments, position tracking and spike sorting was conducted in 2010. During this project, improvements have been done on the spike sorting and position tracking, and times and duration of movement bouts was determined. Perievent time histograms were constructed; using similar histograms from another project as a template and a computer learning program was developed from scratch.

We attended a surgery during 2013, similar to the surgeries done in 2010, to gain insight into all procedures in the project. We have also, for the same reason, been involved in the first steps of the electrode building.

7.2 Pre-analysis

Complications can arise following surgery due to inflammation and bleeding. For instance, infection and tissue damage can provoke inflammation. It is therefore of great importance to maintain a clean and sterilized surgery environment. It is also important that the equipment used during stereotactic surgery is stabilized and does not move unexpectedly in its positioning which would make it more difficult to position the electrodes in the right region. Due to these difficulties, the recordings of neural activity might not always be exactly in the right places. Consequently, histological examination is made post mortem to evaluate were recordings are from.

A primary aim in this research study has been to get neural data which is mainly connected with locomotion. Not much is known about the connections between neural signals on locomotion and other neural signals which might have impact of locomotion. Therefore, distractions have been removed in the experimental environment. The open field environment is relatively devoid of external stimuli (such as odors, movements, sound, etc.) and most of the experiments were made during night time, which is also the time when rats are most active. Nevertheless, neuronal activity relating to ongoing internal processes will still exist but can usually be removed by averaging over multiple trials.

Another aim in this study has been to identify locomotion signals on the neuronal level. However, in reality neuronal activity is probably different, depending

on kinematic differences like acceleration, deceleration, turning right/left or going upwards/downwards. The focus has mainly been on analysing the data around start and stop of locomotion but, it would surely be interesting to also see what is hidden in the neural information if the data is sorted after different locomotion behaviors and thereafter analysed. One suggestion is to develop a labyrinth environment were the rat can choose to move right, left or forward. This might also make the rat more comfortable in the aspect that it prefers to be close to the wall and not in the middle of a free space (see Figure 6.3) and maybe the rat will be more willing to move during an experiment. This way however, we would no longer have the additional opportunity of being able to study how the animal can make use of distant cues in order to build a representation of space (getting to know the area), which is a secondary goal in this set of experiments for NRC. Thus the labyrinth might be effective for this particular experiment but would decrease the diversity of the open field environment.

In the current design, the spontaneous movement bouts are quite few per experiment in spite of the long experiment time. One way this could be improved by forcing the rat to move, but then we would no longer be studying spontaneous voluntary motor behavior. The risk of doing that might be that the signals found might actually be correlated to whatever forsed the rat to start moving rather than the actual movement. Another way to make the rat move more during the experiments could be to make it more used to exercise. A common knowledge for us humans is that the more a person is used to exercising the more they want to move and exercise. This knowledge could perhaps also be applied to rats. A more effective way however, would be to food deprive the animals prior to experiments, and distribute small food pellets in the entire arena.

In the neuronal recordings, an interesting aspect would of course be to not only measure in the regions of the striatum and motor cortex but also in other regions involved in motor control. To obtain parallel recordings from more structures without decreasing the number of channels per structure, poses the need to further develop the electrodes. This is something that is currently being researched at NRC. Also, it would be beneficial to develop electrodes which can record from a single neuron at a time that can then be followed during several experiments. The size of the electrodes used and noise from biological processes and movements makes this task difficult but hopefully this will be possible in the future.

7.3 Spike Sorting

As discussed in the chapter 6, it is often the case that action potentials from more than one neuron is recorded at the same time in a single channel. In the spike sorting procedure neurons are separated from noise and from each other but, given that the noise is evenly distributed it could be argued that the separation from noise is less important for the computer learning as the model should take that into account. However, incorporating more noise would require larger training sets and prolong the computation time. If two neurons have very similar spikes; these will be hard to separate, resulting in a multi-unit. If only one of the neurons are correlated to movement this can dilute the signal, making it harder to use for

prediction. If both neurons are inversely correlated they could cancel each other's signals. However, the different neurons might alternatively amplify and make the signal clearer. In the following step, neuron type is assigned based on the shape of the waveform. Classifying neuron types solely based on their waveform is still somewhat controversial but it has been done in a couple of previous studies and is considered an accepted practice by several researchers now. The waveform features found for the different neuron classes in the current study are close to what have previously been found [Halje et al., 2012]. Overall, there are almost 20 times more MSNs in the striatum than FSIs (see Table 6.2), but this difference is not represented in the number of identified neurons in this study. This might be because the MSNs have significantly lower firing rate than the FSIs and are therefore, more difficult to detect. Another reason might be that the concentration of FSIs in the striatum varies with location and is especially high in the area which are measured from as has been suggested [Berke et al., 2010].

7.4 Video Tracking

The video tracking in the current set-up is in many ways superior to other research departments in neuroscience, which has been an advantage in the current project since it enables to track even minor changes in kinematics of freely moving animals. This shows the importance of involving persons with different fields of expertise in technically challenging experimental disciplines. In this case, in depth knowledge in image analysis had been a prerequisite for the development of the system used.

An experimental challenge in the video tracking procedure has been the constant movements of the cable connected to the rat that transmits the neural data. The cable is often hanging in front of the camera, thus obscuring the rat and making it impossible to track the rat. This is the reason why there exists untracked position and velocity bouts in Figure 6.7 and 6.6 These two figures show data from image points from the head. As mentioned in chapter 5.6.2 there are three positions marked and tracked on the rat: head, body and rear. This can be useful to eliminate missing position data due to cable movement in front of camera but has not been employed in the current analyses. The position and velocity in Figure 6.7 and 6.6 could be supplemented so the empty data in the calculated velocity are estimated either using interpolation from the frames were head position data exists or alternatively be filled in using information from the velocity of the body/rear points. Interpolation can then be made using standard techniques for example linear polynomials/splines. There were occasions where it was difficult to determine if a movement bout should be split into two separate bouts. It is not uncommon for the rat to slow or pause briefly when moving (see Figure 6.6). Generally, such movement with a brief stop was classified as one long bout to improve the baseline (see the discussion below about the baseline of the perievent time histogram).

Tracking takes a lot of time, therefore, only the times around each bout was tracked and at all other times the velocity is assumed to be zero.

In the analyses performed in this project, it was realised that it is difficult to track the rat with only one camera (positioned above the rat). NRC is therefore,

planning to install complementary color cameras providing a side-view of the open field.

7.4.1 Perievent Time Histogram

Because the baseline of the histograms were calculated from the summed firing rates during the corresponding time period in all bouts, the information about the individual bouts are lost. The baseline might potentially be improved by normalising the firing rate of each event before summation. Another problem is that the rat often moves in short bouts, one shortly after another. This means the baseline, to some degree, is contaminated by other bouts which counteract the purpose of the baseline (separating the firing rate during the event from the neuron's normal firing rate). One workaround could be to recalculate the baseline using only the bouts that is not directly preceded by another bout. The drawback of the workaround would be that the baseline become the mean of only a few time periods if a lot of the bouts are close to each other.

The histograms show that neurons correlated to movement can generally be said to either increase or decrease their activity during the movement. Using this criterion, few if any neurons were clearly correlated to only the initialisation or termination of movement were found. There were, however, some neurons that were active only during certain parts of the movement, and it could be interesting to find exactly what the neurons are correlated to. For instance, if they are correlated to movement behavior such as acceleration and retardation.

A visual inspection of the perievent time histograms indicated that 20 neurons was correlated to movement behavior (see Table 6.4). This is quite few neurons which could be due to several factors such as too strict spike sorting, too much biological noise or that the electrodes did not measure in a region with a lot of active neurons. Even though only 20 neurons was visually correlated there might be more neurons correlated to movements if another, more trustworthy, method would be used to find correlated and uncorrelated neurons.

An interesting result in our analyses was that there were significantly more neurons clearly correlated to movement behavior found in the striatum than in the motor cortex, based on the visual inspection of the perievent time histograms. However, it is important to remember this conclusion is only true for the neurons found in this sample. A more rigorous analysis will be needed to define appropriate statistical criteria for what is classified as significant modulations.

7.4.2 Computer learning

The computer learning was able to predict movement with a reasonable accuracy but choosing what configuration of bin size, number of lags and threshold to use is not easy. When evaluating the results in Figure 6.11, there are several points to keep in consideration. The top left of Figure 6.11 (a) shows $1 - FPR$ for the training data set, which was used to set the threshold for the evaluation which is why it is close to constant to 0.99. The $1 - FPR$ for the test data set decreases as the model becomes more overtrained. The TPR evaluation for the training data set indicates that it gets better the more neural data is used (down and right in

the figure). This is also due to overtraining and is not true for the test data set. In (b) the area under the ROC curve is used instead of the TPR and FPR at one point in the curve, this gives a good overview of how good the configuration is generally. The drawback is the unclearness of how well it performs at a specific threshold.

The model used in this project was one of the simplest possible. Thus, it is reasonable to assume it might be possible to improve performance further by choosing a more complex model. Another improvement of performance might be to remove the neurons labeled as not trustworthy. They were left in the data set as the model should be able to handle them but this added noise which might worsen the prediction and needlessly increase the computation time.

The weights in the A-matrix should contain information about neurons correlated to movement. It would be of great interest to evaluate if the model in greater extent favors the neurons which are manually classified as correlated than those which were manually classified as uncorrelated to movement.

The maximum allowed FPR selected in this project was extremely low. It needs to be very low to be feasible to use in a future real world application. if it would not be as strict, a wheelchair controlled by neural signals might start to move on its own without the user intention.

The most time-consuming part of the computer learning algorithms a flaw in the implementation of the model resulting in unreasonably long time periods of neural data seemed to produce the best predictions. This caused a lot of thought as a physiologically more plausible time frame, including only the most recent changes in neurophysiological activity patterns preceding each event should give better predictions. We realised, however, the reason for this counter-intuitive finding was a type of overfitting; meaning the training is specialised for this data set which implicate a very bad performance when confronted with new data. Normally the cross-validation would prevent any overfitting but two combined factors made the cross-validation less sensitive to this error. Firstly, the different cross validation sections were drafted at random from the rows of the X and Y matrices. Thus, it is much more likely there were a number of samples from every movement bout in each of the sections. Secondly, given that these samples were only separated by 120 ms, the rows in the X-matrix corresponding to adjacent samples should be nearly identical for bin sizes much larger than 120 ms (see Figure 5.13, where the opposite case for a bin size less than 120 ms is illustrated). This means the training data and the test data looked nearly identical (see Figure 7.1) which in turn makes it possible to overfit the model despite of the cross validation. This is easily fixed by not separating one movement bout into different crossvalidiation sections, and also by making a more careful selection of reasonable bin sizes. Also, the false negative rate should be evaluated in addition to the true positive rate when evaluating the performance of the computer learning. It is likely that other researchers may have fallen into the same pitfall and can be helped by this realisation. Therefore, we recommend it should be clearly stated in future studies, with the use of the current design, that great care must be taken when the data sets is separated into different behavioral events. Due to the long time of the recording, there is a lot of data to analyse in the training. So much so the computer could not handle the large matrix operations. This led to the data being down sampled by a factor three (one frame

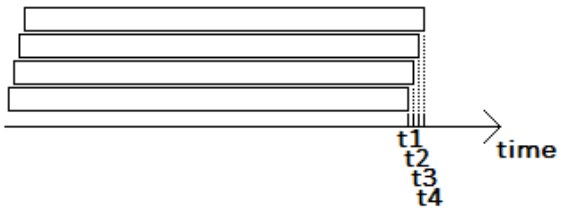

Figure 7.1: *Example of why the adjacent bins are nearly identical if they are much larger than the time between observations.*

in three was used during the computer learning). Even after down sampling the X-matrix had 260000 rows, and almost 1000 columns for the configurations with the most lags. This pushed the computer to the limit and would have required more than the available 8GB of RAM to compute a configuration with more lags.

7.5 Future Research

There are a lot of interesting possibilities for future research building on this project. Some of the ideas for improvements and related work could be to include the local field potential into the model for prediction. The LFP is the synchronous activity of groups of neurons. It would be interesting to predict more specific aspects of the movements, like movement direction, speed, acceleration, turning, body angle, angular velocity and angular acceleration. Moreover, it could also prove useful to have neural information from other regions in the brain that are known to be involved in movement.

Most importantly, we suggest the current approach could be used to learn more about how different neuron assemblies contribute to motor control, essentially allowing for a new approach to neurophysiological research where the investigator may use machine learning techniques to understand complicated physiological processes.

Chapter 8
Conclusions

Neurons correlated to movement have been found in both the motor cortex and striatum but there are more correlated neurons in the stratum than in the motor cortex ($p < 0.05$). Although, the method for determining correlation needs to be improved before the significance can be said to be truly trusted.

Generally, the neurons seem to be correlated to the entire movement and not only to the initialisation or termination. There are, however, neurons whose firing rate differs depending on where in the movement bout the rat is. More research is needed to determine why and what it is correlated to.

During the computer learning a major pitfall was found and corrected. Hopefully others can benefit from this by not making the same mistake. The neurons' firing rate can be used to predict when the rat moves with relatively good precision.

Chapter 9
Scientific Setting

Neuronano Research Center (NRC) is an interdisciplinary research center with the goal to develop neural interfaces that communicates with the nervous system. NRC contains of five platforms: neural probes; biocompatibility; data aquisition, encoding, telemetry and analysis; neuroscience research and clinical applications; and etics. The vision is to "... improve quality of life for disabled people and individuals with neurodegenerative disorders by listening to, understanding and talking to the nervous system by means of a neural interface".[NRC]. Out of these three objectives, this study falls within the secondary category of understanding the nervous system.

Professor Jens Schouenborg is the coordinator of NRC and the research group consists of researchers from the Faculties of Engineering, Humanities, Medicine and Science.[NRC]

NRCs' neuroscience research is done both in vivo and in vitro combined with nano- and microtechnology. The research group is frequently going to neuroscience conferences to get an updated view of the cutting-edge research of the nerve system and the brain. We, Moa and Joel, have had the honor to be part of this research environment, as well as participating in a five days inspirational conference held in San Diego. The Society for Neuroscience (SfN) arranged a gathering for thousands of neuroscientists to participate in the newest research areas, which were presented with seminars, poster discussions, networking and workshops [SfN].

Chapter 10
Acknowledgements

People within Neuronano Research Center have given us an interesting view within this study. We would like to thank our supervisors Ulrike Richter and Per Petersson who have both devoted a lot of time to this study and given us great inputs and support. We would also like to thank Pär Halje, who has given us more information about the MATLAB toolboxes used at Neuronano Research Center; Martin Tamtè for his expertise within neural sorting; Nedjeljka Ivica for her surgical expertise; Maruf Ahmed for his special knowledge within electrode development; and Veronica Johansson for her ethical inputs. Not to mention our test readers Mikael Rudner and Katherinne Smythe who have improved the script by given us valuable comments.

Chapter 11
Glossary

Action Potential a depolarization of a cell membrane. It is triggered when the critical threshold is reached. This is also called a spike.

Axon a nerve fiber which sends out electrical impulses from the neuron nucleus.

Basal Ganglia located at the base of the brain. This region is involved in the process of voluntary movement among other tasks.

Brain Machine Interface a communication pathway between a device and the brain.

Cell Body see soma

Cortico-Striatal Activity neural activity (signals) from the cortex to the striatum.

Cortex located at the outer region of cerebral hemisphere.

Dendrite a nerve fiber of the neuron which receives electro-chemical impulses from other neurons.

Electroencephalography can be used to do non-invasive recordings of neural activity.

Excitatory Neuron a neuron that excites the neurons it projects to. See also inhibitory neuron.

Fast Spiking Interneuron a type of neuron with axons projecting to local neurons (in the same region). One of its characteristics is its fast firing rate.

Firing Rate the rate at which the neuron fires its action potentials (Hz).

Functional Magnetic Resonance Imaging Measures neural activity by detection of changes of blood flow.

Glial Cell has different functions depending on what type it is. For instance, one type can regulate the internal surroundings around the neurons while another one forms myelin and protects and stabilizes the neurons. Glial cells can also supply oxygen and nutrition or destroy microorganisms and clean up dead neurons.

Gray Matter consists of neuron nucleus, dendrites and unmyelinated axons.

Inhibitory Neuron a neuron that inhibits the neurons it projects to. See also excitatory neuron.

Interneuron a neuron which connects other neurons to each other.

Inter-Spike Interval The time between the neural firing.

Medium Spiny Neuron an inhibitory neuron which regulates the neurons' activation. MSN exists in the striatum and is active both within the striatum and regions connected with the striatum. The major functions of MSN are environmental recognition and encoding of locomotion.

Medulla Oblongata connects the signals from the rest of the brain to the spinal cord hind brain.

Multi Units clusters of action potentials which are identified to come from more than one neuron.

Myelin covers the axons. Myelin improves the propagation speed of the action potentials.

Neuralynx a data recording system for electrophysiology signals.

Neuron also called a nerve cell. It consists of a neuron nucleus, axons and dendrites

Neuroprosthesis a mind-controlled prosthesis.

Nerve Cell see neuron.

Nerve Impulse neural activity.

Offline Sorter a program used to classify action potential waveforms (spikes) which are collected from electrodes. The spikes can be seen in 2D or 3D feature space. Different clustering techniques exist and cluster separations can be calculated.

Postsynaptic Potential is a graded potential which is created by membrane potential changes of the postsynaptic terminal and its function is to inhibit or initiate action potentials.

Pyramidal Neuron exists in the cerebral cortex, hippocampus and amygdala. A pyramidal neuron can be classified in different subclasses depending on firing rate. Pyramidal neurons can connect their axons both within the region but also to distant regions.

Refractory Period occurs after an action potential is generated. The refractory period is the time interval in which a second action potential cannot be applied until the voltage has returned to its resting state.

Single Unit clusters of action potentials which are identified to come from only one neuron.

Soma also called cell body or a cell nucleus. This is where the protein synthesis occurs.

Spike an action potential.

Striatum located in basal ganglia. Voluntary motion is processed in this region.

Substantia Nigra located in basal ganglia. It plays a role in addiction, reward and movement.

Subthalamic Nucleus located in basal ganglia. The function is unknown.

Synapse is the structure between neurons which allows chemical and electrical signals to pass between neurons.

Synaptic Membrane Potential refers to the neurons incoming signal which is the voltage difference between the inside and outside of a postsynaptic neuron's membrane. The synaptic potential can be either inhibitory or excitatory.

Thalamus located in the forebrain. The thalamus is known to be a sensory relay station where sensory information is processed and relayed to the motor cortex.

Threshold Potential the critical depolarization level of the membrane potential in order to start an action potential.

White Matter consists of glial cells and myelinated axons.

Chapter 12
Acronyms

BMI Brain Machine Interface

EEG Electroencephalography

EPSP Excitatory Post-Synaptic Potential

IS Excitatory synapse

IN Interneuron

IS Inhibitory synapse

ISI Inter-Spike Interval

IPSP Inhibitory Post-Synaptic Potential

FPR False Positive Rate

FSI Fast Spiking Interneuron

fMRI Functional Magnetic Resonance Imaging

GPe Globus Pallidus external segment

GPi Globus Pallidus internal segment

MSN Medium Spiny Neuron

MU Multi Units

NRC Neuronano Research Center

PN Pyramidal Neuron

ROI Region Of Interest

SU Single Unit

STN Subthalamic Nucleus

TPR True Positive Rate

UIN Unidentified

Chapter 13
References

Ammar Al-Chalabi, R. Shane Delamont, and Martin R. Turner. *The Brain: A Beginner's Guide (Beginner's Guides)*. Oneworld Publications. ISBN 1851685944. URL http://www.amazon.com/The-Brain-Beginners-Guide-Guides/dp/1851685944.

Jose M Carmena, Mikhail A Lebedev, Roy E Crist, Joseph E O'Doherty, David M Santucci, Dragan F Dimitrov, Parag G Patil, Craig S Henriquez, and Miguel A L Nicolelis. Learning to control a brain-machine interface for reaching and grasping by primates. *PLoS biology*, 1(2):E42, November 2003. ISSN 1545-7885. doi: 10.1371/journal.pbio.0000042. URL http://dx.plos.org/10.1371/journal.pbio.0000042.

CODEX. CODEX - regler och riktlinjer för forskning. URL http://www.codex.vr.se/forskningdjur.shtml.

Tom Fawcett. An Introduction to ROC Analysis. *Pattern Recogn. Lett.*, 27(8): 861–874, 2006. ISSN 0167-8655. doi: 10.1016/j.patrec.2005.10.010. URL http://dx.doi.org/10.1016/j.patrec.2005.10.010.

Gamry. Home - Gamry Instruments. URL http://www.gamry.com/.

Pär Halje, Martin Tamtè, Ulrike Richter, Mohsin Mohammed, M Angela Cenci, and Per Petersson. Levodopa-induced dyskinesia is strongly associated with resonant cortical oscillations. *The Journal of neuroscience : the official journal of the Society for Neuroscience*, 32(47):16541–51, November 2012. ISSN 1529-2401. doi: 10.1523/JNEUROSCI.3047-12.2012. URL http://www.ncbi.nlm.nih.gov/pubmed/23175810.

Integrative Neurophysiology. Integrative Neurophysiology | Medicinska fakulteten, Lunds universitet. URL http://www.med.lu.se/english/expmed/research/intergrative_neurophysiology.

Moa Svensson and Joel Sjöbom. Complementary Figures, 2014. URL http://eje.mine.nu/master_thesis_decoding_motor_commands/complementary_figures.pdf. Online; accessed 13-February-2014.

NRC. NRC - Neuronano Research Center | Medicinska fakulteten, Lunds universitet. URL http://www.med.lu.se/nrc.

George Paxinos and Charles Watson. *The Rat Brain in Stereotaxic Coordinates, Sixth Edition*. Elsevier Books, 2007. ISBN 0125476124. URL http://www.amazon.com/Brain-Stereotaxic-Coordinates-Sixth-Edition/dp/0125476124.

Dale Purves, George J. Augustine, David Fitzpatrick, William C. Hall, Anthony-Samuel Lamantia, James O. McNamara, and S. Mark Williams.

Robert Schmidt, Daniel K Leventhal, Nicolas Mallet, Fujun Chen, and Joshua D Berke. Canceling actions involves a race between basal ganglia pathways. *Nature neuroscience*, 16(8):1118–24, August 2013. ISSN 1546-1726. doi: 10.1038/nn.3456. URL http://dx.doi.org/10.1038/nn.3456.

SfN. Society for Neuroscience - Highlights. URL http://www.sfn.org/annual-meeting/neuroscience-2013/.

Hagar G Yamin, Edward A Stern, and Dana Cohen. Parallel processing of environmental recognition and locomotion in the mouse striatum. *The Journal of neuroscience : the official journal of the Society for Neuroscience*, 33(2):473–84, January 2013. ISSN 1529-2401. doi: 10.1523/JNEUROSCI.4474-12.2013. URL http://www.ncbi.nlm.nih.gov/pubmed/23303928.

LUND
UNIVERSITY

http://www.eit.lth.se